ORIGINAL RESEARCH ARTICLE

CrossMark

Combining Ibrutinib with Chk1 Inhibitors Synergistically Targets Mantle Cell Lymphoma Cell Lines

Valentina Restelli[1] · Monica Lupi[1] · Micaela Vagni[1] · Rosaria Chilà[1] · Francesco Bertoni[2,3] · Giovanna Damia[1] · Laura Carrassa[1]

Abstract

Background Mantle cell lymphoma (MCL) is an aggressive B cell lymphoma with an unfavorable clinical course. Besides deregulation of the cell cycle, B cell receptor (BCR) signaling, essential for MCL proliferation and survival, is also often deregulated due to constitutive activation of Bruton's tyrosine kinase (BTK). The BTK inhibitor ibrutinib has been approved as a therapy for refractory MCL, and while it shows some clinical activity, patients frequently develop primary or secondary ibrutinib resistance and have very poor outcomes after relapsing following ibrutinib treatment.

Objective To overcome ibrutinib resistance, new therapeutic approaches are needed. As checkpoint kinase 1 (Chk1) inhibitors have recently been shown to be effective as single agents in MCL, we assessed the combination of ibrutinib with Chk1 inhibitors.

Methods We examined the activity of ibrutinib combined with the Chk1 inhibitor PF-00477736 in eight MCL cell lines and analyzed underlying cellular and molecular effects.

Results The combination was synergistic in all tested cell lines through different mechanisms. The treatment induced apoptosis in ibrutinib-sensitive cell lines, while in ibrutinib-resistant cells the effect was mainly cytostatic and occurred at micromolar concentrations of ibrutinib.

Conclusions The pharmacological approach of simultaneously targeting cell cycle checkpoints (by Chk1 inhibitors) and pro-survival pathways (by ibrutinib) might offer a promising new therapeutic strategy for MCL patients.

✉ Giovanna Damia
giovanna.damia@marionegri.it

✉ Laura Carrassa
laura.carrassa@marionegri.it

[1] Laboratory of Molecular Pharmacology and Laboratory of Cancer Pharmacology, Department of Oncology, IRCCS-Istituto di Ricerche Farmacologiche "Mario Negri" (IRFMN), via La Masa 19, 20156 Milan, Italy

[2] Institute of Oncology Research (IOR), Università della Svizzera Italiana (USI), Bellinzona, Switzerland

[3] Oncology Institute of Southern Switzerland (IOSI), Bellinzona, Switzerland

Key Points

Targeting pro-survival pathways by using the BTK inhibitor ibrutinib, and the cell cycle checkpoint pathway by using the Chk1 inhibitor PF-00477736, is synergistic in MCL cell lines.

Combining ibrutinib with Chk1 inhibitors could be of therapeutic benefit in MCL patients.

This new combined approach has the potential to be translated into the clinical setting for the treatment of MCL.

1 Introduction

Mantle cell lymphoma (MCL) is a rare, aggressive B cell lymphoma with an unfavorable clinical course and a median overall survival of 4-5 years. Since MCL is not curable with current therapies, new therapeutic strategies are urgently needed. Cell cycle deregulation due to the chromosomal translocation t(11;14) leading to over-expression of cyclin D1 is a pathogenic hallmark of MCL. This is almost invariably accompanied by additional alterations in genes regulating DNA damage response and cell cycle pathways (such as *MYC*, *ATM*, *p53*, and *CDK4*). Besides deregulation of the cell cycle, MCL also encompasses secondary genetic events that enhance cell growth, activate cell survival pathways, and inhibit apoptosis [1–5]. B cell receptor (BCR) signaling is essential for the proliferation of MCL, and is often deregulated due to the over-activation of kinases such as Bruton's tyrosine kinase (BTK), which acts upstream of important transcriptional pro-survival pathways (e.g., MEK/ERK, p38MAPK, NF-κB [nuclear factor-κB], and JAK/STAT3) [6–8]. Ibrutinib, a potent inhibitor of BTK, has recently been approved for the treatment of refractory MCL on the basis of impressive clinical responses [9]. However, despite this unprecedented clinical activity, about one-third of MCL patients do not respond to ibrutinib and many others eventually develop secondary resistance [10, 11].

Some mechanisms of ibrutinib resistance have been identified. The point mutation C481S in the ibrutinib binding site of BTK is the best known cause of acquired resistance to ibrutinib and generally occurs at relapse, after prolonged exposure to the drug [12]. However, this mutation is not detected in patients with primary resistance to ibrutinib or patients that develop early resistance. MCL cell lines primarily resistant to ibrutinib are dependent on the alternative NF-κB signaling pathway, which are not mediated by BTK. These cells have mutations in genes implicated in the negative regulation of this pathway, which were also found in approximately 17% of 165 primary MCL samples (e.g., mutations in *TRAF2*, *TRAF3*, and *MAP3K14*) [13]. MCL cell lines with constitutive activation of the alternative NF-κB pathway are resistant to ibrutinib [11, 13]. Primary ibrutinib resistance in MCL may also depend on sustained PI3K–AKT pathway activation, which recently provided the rationale for combining PI3K–AKT inhibitors with ibrutinib [10, 12]. The unrestrained proliferation of relapsed MCL cells after ibrutinib treatment suggests that simultaneous targeting of cell cycle regulators may delay the expansion of resistant clones or override some mechanisms of resistance [12].

We recently provided evidence that checkpoint kinase 1 (Chk1) inhibitors are cytotoxic in cyclin D1-driven MCL cells [14]. MCL cells with the t(11;14) translocation have an enhanced G1-S transition, meaning that they rely more on Chk1 for survival since this kinase is vital for the initiation of DNA replication and for the correct progression into S phase, minimizing endogenous DNA damage [14]. Lymphoma cells with both primary or secondary resistance to Chk1 inhibitors have been shown to be enriched in genes of pro-survival and proliferative pathways [14, 15].

In this study we explored a combination approach of Chk1 inhibitors with ibrutinib in MCL. Co-treatment with the Chk1 inhibitor PF-00477736 and ibrutinib in vitro had a synergistic effect in eight MCL cell lines that are sensitive or resistant to ibrutinib. Apoptosis occurred in ibrutinib-sensitive cell lines, while in ibrutinib-resistant cell lines the effect of the drug combination was mainly cytostatic and occurred at high ibrutinib concentrations. These data can provide the basis for a new combined pharmacological approach in MCL by interfering with cell cycle checkpoints and pro-survival pathways, which could be translated to a clinical setting.

2 Methods

2.1 Cell Culture and Drugs

MCL cell lines REC-1, SP-49, MINO, JEKO-1, MAVER-1, GRANTA-519, JVM2, and JEKO-1 R were maintained in RPMI 1640 Medium supplemented with 1% glutamine, 1% penicillin/streptomycin, and 10% fetal bovine serum (FBS). Cells were cultured at 37 °C in 5% CO_2. The cell lines were kindly provided by different groups, as previously specified [14]. The JEKO-1 R cell line resistant to the Chk1 inhibitor PF-00477736 was obtained as previously described [15]. All cell lines were authenticated by the authors in the last 6 months. The short tandem repeats (STR) profiles were compared with the American Type Culture Collection database or to the German Collection of Microorganisms and Cell Cultures database.

The Chk1 inhibitors PF-00477736, AZD-7762 (both from Axon Medchem, Groningen, The Netherlands), and GDC-0575 (Active Biochem, Kowloon, Hong Kong) and the BTK inhibitor ibrutinib (Axon Medchem, Groningen, The Netherlands) were all dissolved in dimethyl sulfoxide (DMSO) in stock solution of 10 mM and stored at −20 °C.

2.2 Drug Treatments and Viability Tests

The effect of each drug on cell growth both as a single agent and in combination was determined using the MTS (3-(4,5-dimethylthiazol-2-yl)-5-(3-carboxymethoxyphenyl)-2-(4-sulfophenyl)-2H-tetrazolium) assay. Cell lines were seeded in 96 well plates and treated after 48 h with ten serial concentrations of each drug (Electronic Supplementary Material Table 2 summarizes the concentration of cells seeded for each cell line). MTS reagent (Promega, Milan, Italy) was added to each well after 96 h of treatment. Cell proliferation was evaluated using a plate reader (Infinite® M200, TECAN, Männedorf, Switzerland). The 50% inhibitory concentration (IC_{50}) values

of the compounds for each cell line were calculated with Calcusyn Software (Biosoft, Cambridge, UK). For the assessment of the combined treatment, each cell line was treated simultaneously with serial concentrations of PF-00477736 and ibrutinib. Results were examined by isobologram analysis with Calcusyn Software and Combination Index (CI) values at the IC_{50} were calculated to evaluate the efficacy of the combination [14, 16]. To study the cellular and molecular effects exerted by the drug combinations, ibrutinib-sensitive MINO and ibrutinib-resistant MAVER-1 cells were seeded in T25 flasks. Two days later, cells were either left untreated or treated with ibrutinib and PF-00477736 (MINO cells: ibrutinib 10 nM and PF-00477736 30 nM; MAVER-1 cells: ibrutinib 2 μM and PF-00477736 15 nM). We chose the lower concentration of both drugs able to produce a strong cytotoxic effect. The growth of the cells was followed for 96 h by counting them (three T25 flasks per group) every 24 h using the Multisizer™ 3 Coulter Counter® (Beckman, Milan, Italy) and evaluating their concentration as number of cells/ml (all samples were cultured in the same volume). Part of these cells were fixed for flow cytometric analysis at the described timepoints and/or proteins and RNA were extracted for molecular investigations described in the following sections.

2.3 Western Blotting Analysis

Proteins were extracted and visualized using standard techniques as previously described [17]. Primary anti-Chk1 (1:500, cat.#sc-8408), Erk (1:500, cat.#sc-94), pY204-Erk (1:500, cat.#sc-7383), and actin (1:500 cat.#sc-1616) were purchased from Santa Cruz Biotechnology (Heidelberg, Germany). Primary anti-pS317-Chk1 (1:1000, cat.#2344S), pY223-Btk (1:500, cat.#5082S), and pT68-Chk2 (1:1000, cat.#2661S) were purchased from Cell Signaling Technology (Danvers, MA, USA). Primary anti-BTK (1:500, cat.#ab32555) was purchased from Abcam (Cambridge, MA, USA). The anti-γH2AX (1:1000, cat.#05-636) antibody was purchased from EMD Millipore (Burlington, MA, USA). The anti-Chk2 (1:500, cat.# K0087-3) antibody was purchased from MBL Life science (Woburn, MA, USA).

Secondary HRP (horseradish peroxidase)-conjugated antibodies anti-goat (sc-2020), anti-rabbit (sc-2004), and anti-mouse (sc-2005) were purchased from Santa Cruz Biotechnology.

2.4 Flow Cytometric Analysis

To analyze cell cycle distribution by flow cytometry, MINO and MAVER-1 cells were fixed in 70% ethanol 24, 48, and 72 h after PF-00477736 and ibrutinib treatments either singly or combined and processed as previously described [17]. Cell cycle percentages in the different phases were obtained by flow cytometric histograms as previously described [18].

2.5 Caspase-3 Activity and TUNEL Assay

Caspase-3 activity was measured in protein extracts of MINO, MAVER-1, JEKO-1, and GRANTA-519 cells after 24, 48, and 72 h of treatment with an enzymatic assay using a fluorogenic substrate for caspase-3, Ac-DEVD-AMC (acetyl Asp-Glu-Val-Asp 7-amido-4-methylcoumarin), as previously described [16]. DNA fragmentation in MINO and MAVER-1 cells, untreated or treated with PF-00477736, ibrutinib, or the combination, was detected by flow cytometric analysis using the TdT-mediated dUTP nick-end labeling technique (TUNEL) (Roche, Mannheim, Germany) [16].

2.6 mRNA Quantification by Real-Time PCR

Total RNA was extracted from MINO and MAVER-1 cell lines using Maxwell® 16LEV simplyRNA Cells Kit (Promega, Milan, Italy). RNA was reverse-transcribed to complementary DNA (cDNA) using a High Capacity cDNA Reverse Transcriptional Kit (Applied Biosystems, Monza, Italy). Optimal primer pairs were chosen for each gene of interest, using PRIMER-3 software (Electronic Supplementary Material Table 1). Differences in gene expression were determined by real-time PCR (RT-PCR) with SYBR™ Green PCR Master Mix (Applied Biosystems, Monza, Italy) and the dissociation curve was evaluated for each gene. Samples were then normalized using the expression of the housekeeping gene (actin) and their levels were compared with those of control samples. Changes less than 0.5-fold (down-regulated gene) or more than two-fold (up-regulated gene) compared with the control samples were considered significant. RT-PCR was done using the ABI PRSIM®7900HT Sequence Detection System (Applied Biosystems, Monza, Italy).

2.7 Statistical Analysis

Data are expressed as mean ± standard deviation (SD) of at least three replicates and are representative of three independent experiments. Statistical analysis was performed with GraphPad Prism 7.02 (GraphPad Software, San Diego, CA, USA). The statistical tests that were performed are specified in the legends of the figures. $P < 0.05$ was considered statistically significant.

3 Results

3.1 Combined Treatment with Chk1 and BTK Inhibitors is Synergistic in Mantle Cell Lymphoma Cell Lines

We examined the effects of ibrutinib combined with the Chk1 inhibitor PF-00477736 in eight MCL cell lines,

including cell lines that are highly sensitive (REC-1, SP-49), sensitive (MINO, JEKO-1), and primary resistant (MAVER-1, GRANTA-519, and JVM2) to ibrutinib [13], and the JEKO1-R cell line [15] with secondary resistance to PF-00477736 (Fig. 1a). The isobologram in Fig. 1b summarizes the CIs for each cell line at an IC_{50} when the two drugs were combined, showing a synergistic effect (CI < 1) in all cell lines (with CI from 0.48 to 0.7). The synergistic effect was observed irrespective of the cell sensitivity to PF-00477736 and ibrutinib. The combination dose–response curves (Fig. 2a–b and Electronic Supplementary Material Figure 1), suggested that in all the cell lines the activity of ibrutinib was strongly potentiated by low effective concentrations of PF-00477736 (from 6 to 50 times potentiation), with the exception of the highly sensitive cell lines to ibrutinib (SP-49 and REC-1) where the potentiation by PF-00477736 was at most three times. In the ibrutinib-resistant cell lines the synergism is evident with ibrutinib concentrations in the range of 500–2500 nM. A similar synergistic effect was observed by combining ibrutinib with other Chk1 inhibitors (AZD-7762, GDC-0575), both in ibrutinib-sensitive (MINO) and -resistant (MAVER-1) cell lines (Fig. 2c–d).

3.2 Combining Ibrutinib with the Chk1 Inhibitor PF-00477736 Arrests Cell Proliferation and Induces a DNA Damage Response

The ibrutinib-sensitive (MINO) and -resistant (MAVER-1) cell lines were further characterized to elucidate the cellular and molecular effects of the synergy of the combination

(Fig. 3). Cells were treated (as described in the Methods section) with concentrations of the two inhibitors that display a strong synergistic effect when combined. Figure 3a shows the cell growth of the two cell lines every 24 h up to 96 h. There was a slight effect on cell growth only at 96 h after single treatment, but starting from 24 h the combination strongly reduced cell growth for up to 96 h in both cell lines (more than 90% of growth inhibition).

Decreased phosphorylation in Y223 of BTK, a pharmacodynamic parameter of BTK inhibition [19], and increased phosphorylation in S317 of Chk1, a marker of Chk1 inhibition [20], were observed 24 h after the corresponding treatments in both cell lines, suggesting that the concentrations of the inhibitors used as single agents, while only slightly compromising cell growth, were effective in inhibiting their respective targets (Fig. 3b). Inhibition of the two targets was maintained with the combined treatment, excluding any interference. The combination induced a DNA damage response in both cell lines, as indicated by the increase in Chk2 phosphorylation and in γH2AX (phosphorylated at S139), which in MINO cells persisted up to 72 h, while in MAVER-1 cell line it was evident only up to 48 h after treatment (Fig. 3c–d).

3.3 Cell Cycle Perturbation and Apoptosis Induced by the Combination Treatment

No cell cycle perturbations were observed with single drug treatments, while the combined treatment induced different cell cycle perturbations in the two cell lines (Fig. 4a). Specifically, as shown in Fig. 4a (left panel) and in Electronic Supplementary Material Figure 2A, the

a

Cell lines	IC 50(nM)		CI at the IC50 values
	IBRUTINIB	PF-00477736	
SP-49	0.2±0.1	100±13	0.65
REC -1	1.5±0.5	>5000	0.70
MINO	820±25	54±10	0.48
JEKO-1	800±200	15±3	0.52
JEKO-1 R	1340±380	140±15	0.6
JVM-2	2400±1200	60±6	0.68
MAVER-1	6900±1600	25±5	0.51
GRANTA-519	17000±2000	25±0.5	0.50

b

Fig. 1 Synergistic effect of PF-00477736 and ibrutinib in mantle cell lymphoma (MCL) cell lines. **a** Table showing the 50% inhibitory concentration (IC_{50}) values of ibrutinib (BTK inhibitor) and PF-00477736 (Chk1 inhibitor) and the CI at the IC_{50} values of the combination of the two drugs in MCL cell lines. IC_{50} values are represented as mean ± standard deviation (SD) of three independent experiments. **b** Normalized IC_{50} isobologram showing the synergistic
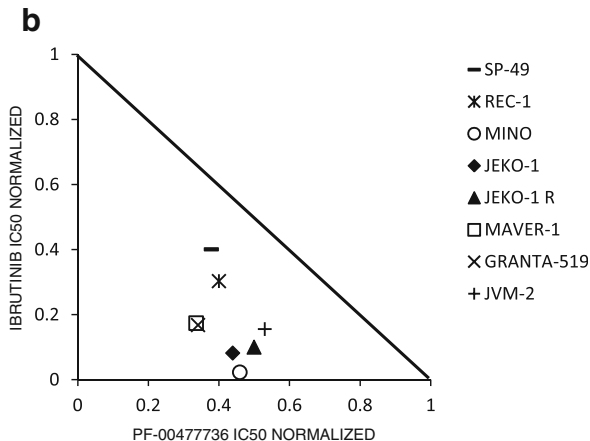
effects of the drug combination in the MCL cell lines. Cells were treated simultaneously with serial concentrations of PF-00477736 and ibrutinib for 96 h and the effect of the drug combination was measured by MTS assay. Results were examined by isobologram analysis. The concentrations of the two drugs exerting 50% antiproliferative effect when combined were normalized to the IC_{50} of the single drugs. The data are representative of three independent experiments
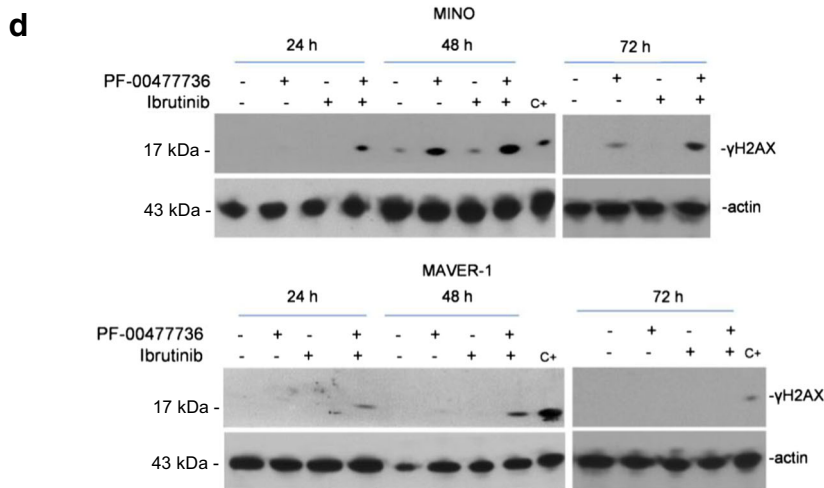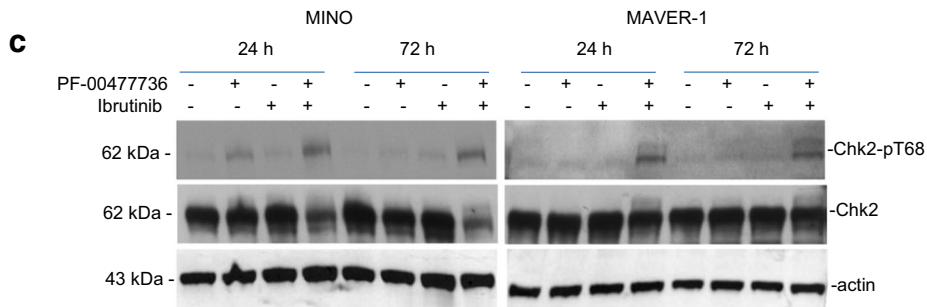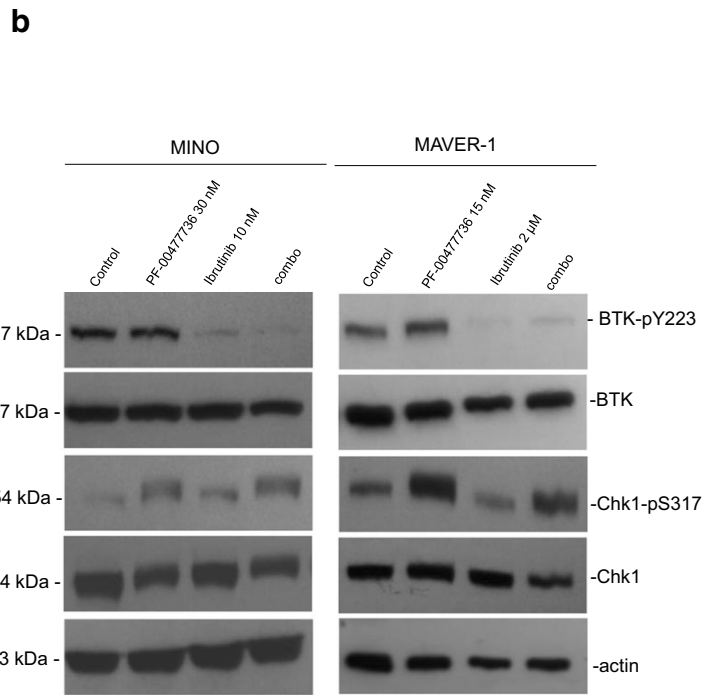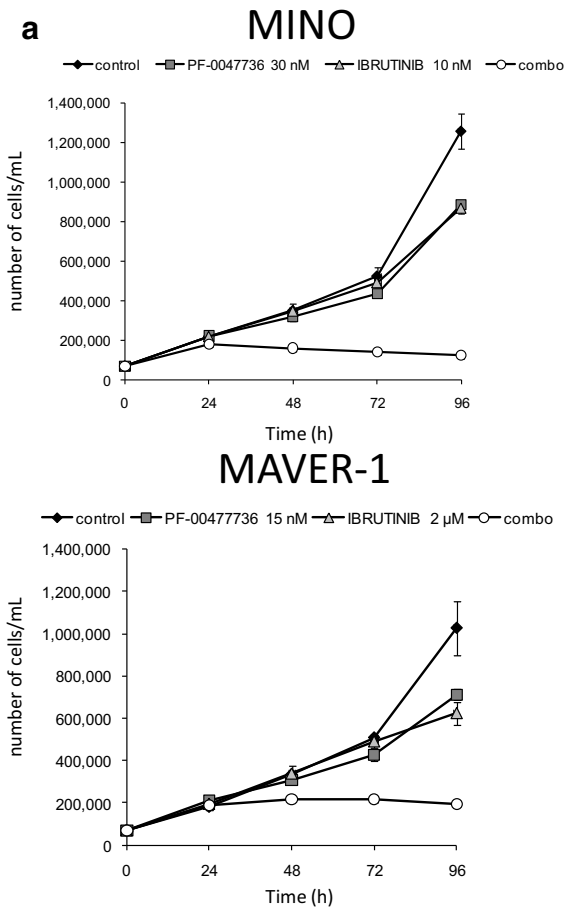
a MINO

b MAVER-1

c

d
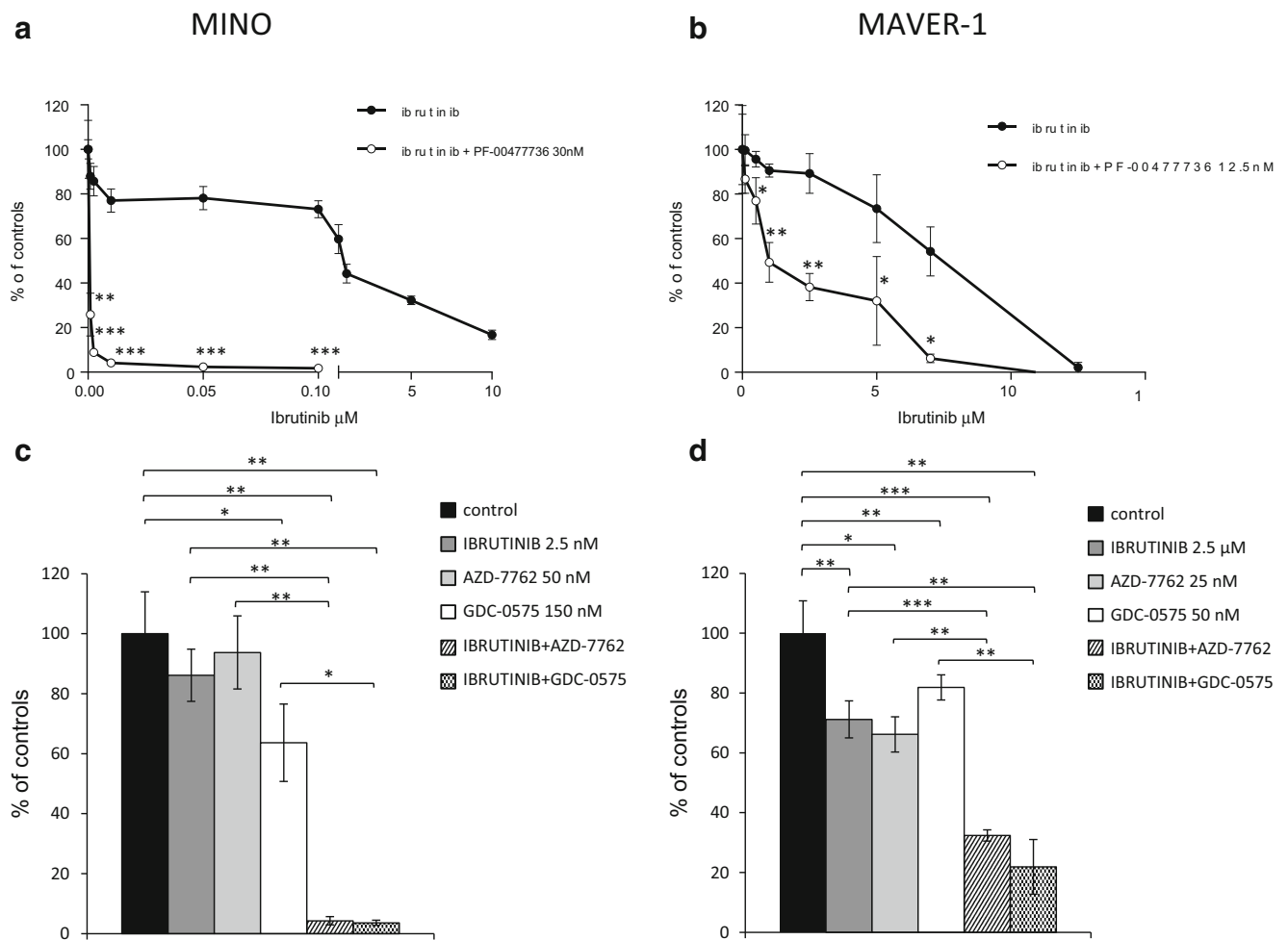
Fig. 2 Ibrutinib combined with Chk1 inhibitors acts synergistically in both ibrutinib-sensitive MINO and ibrutinib-resistant MAVER-1 cells. **a**–**b** Dose–response curves of ibrutinib as single agent or in combination with low effective concentrations (interfering at maximum 15% of cell proliferation) of PF-00477736 in the MINO cell line (**a**) and MAVER-1 cell line (**b**). The data were determined by MTS assay and are representative of three independent experiments and indicate the mean percentage ± standard deviation (SD) of three replicates. The significance of differences between the curves was measured with the Student's t-test

($P < 0.05$ was considered statistically significant). **c**–**d** Histograms showing the synergistic effect of ibrutinib with AZD-7762 and GDC-0575 in MINO (**c**) and MAVER-1 (**d**) cells at concentrations specified in the figure. AZD-7762 and GDC-0575 concentrations used have low effectiveness as single agents. The data shown were determined by MTS assay. They are representative of three independent experiments and are expressed as mean percentage ± SD of three replicates ($P < 0.05$ was considered statistically significant). * $P < 0.05$, ** $P < 0.01$, *** $P < 0.001$

combination caused an increase in the sub-G1 population in MINO cells starting from 24 h and more evident at 48–72 h, suggestive of apoptotic cell death. Moreover, there was an accumulation of cells in early S phase at 72 h, indicating an impairment in the progression through the S phase. Conversely, as shown in Fig. 4a (right panel and in Electronic Supplementary Material Figure 2B), in MAVER-1 cells treated with the combination, no sub-G1 events were observed, and apparently no modification of the cell cycle distribution could be observed. However, considering the fact that cell proliferation was completely inhibited, as highlighted by the growth curves (Fig. 3a), we hypothesized that a 'cell freezing' was indeed occurring. Of note, a slight accumulation

in late S/G2-M could be detected at 48 and 72 h (Electronic Supplementary Material Figure 2B).

In MINO cells the caspase-3 activity in the same experimental conditions (Fig. 4b) indicated apoptosis activation after the drug combination. Although there was a slight increase in caspase-3 activity (about double at 24 h and three times at 48 and 72 h), after PF-00477736 treatment as compared with untreated and ibrutinib-treated cells, the increase was more marked after the drug combination at all timepoints, reaching more than ten times at 24 and 48 h and four times at 72 h after treatment. MAVER-1 cells showed only slight activation of caspase-3 after treatment with the drug combination (Fig. 4b, right panel).

a

MINO

◆ control ■ PF-0047736 30 nM △ IBRUTINIB 10 nM ○ combo

MAVER-1

◆ control ■ PF-00477736 15 nM △ IBRUTINIB 2 μM ○ combo

b

c

d

◀ **Fig. 3** Effects of the drug combination in MINO and MAVER-1 cells. **a** Cell growth curve of MINO (upper panel) and MAVER-1 (lower panel) cells, untreated or treated with the drugs either singly or combined at the concentrations indicated. The data are representative of three independent experiments and are expressed as the mean cell number/ml ± standard deviation (SD) of three replicates (error bars are not visible when smaller than symbols). ANOVA was used for statistical analysis. Statistical significance differences observed are as follows: MINO—48 h: combo vs. all the other groups, *** $P < 0.001$; 72 h: control vs. PF-00477736, ** $P < 0.01$ and combo vs. all the other groups, *** $P < 0.001$; 96 h: control vs. all the other groups, *** $P < 0.001$ and combination (combo) vs. single agents, *** $P < 0.001$; and MAVER-1—48 h: combo vs. control and ibrutinib, ** $P < 0.01$ and combo vs. PF-00477736, * $P < 0.05$; 72 h: combo vs. all the other groups, *** $P < 0.001$; 96 h: control vs. all the other groups, *** $P < 0.001$ and combo vs. single agents, *** $P < 0.001$. **b** Western blot analysis showing pY223-BTK, BTK, pS317-Chk1, Chk1, and actin protein levels as pharmacodynamic parameters of and Chk1 inhibition in MINO (left panel) and MAVER-1 (right panel) cell lines. Ibrutinib abrogates the activation of BTK by inhibiting its autophosphorylation at Tyr-223 [19]; the Chk1 inhibitor abrogates the continuous dephosphorylation of Chk1 by inhibiting the phosphathase PP2A, which is positively regulated by Chk1 [20]. **c** Western blot analysis showing pT68-Chk2, Chk2, and actin protein levels in MINO (left) and MAVER-1 (right) cell lines after 24 and 72 h of treatment with the two drugs either alone or combined at concentration exerting less than 20% of cytotoxicity as single agents and synergistic when combined. **d** Western blot analysis of γH2AX and actin protein levels in MINO (upper panel) and MAVER-1 (lower panel) cells after 24, 48, and 72 h of treatment with the two drugs either singly or combined. γH2AX-positive protein extracts were included, represented by JEKO-1 R treated with PF-00477736 150 nM [15]. **b**–**d** are representative of three biological replicates

In line with these observations, the TUNEL assay performed at 72 h after treatment showed a strong increase in the percentage of cells with fragmented DNA after the drug combination (45%) in MINO cells while only a marginal increase (15%) was observed in the sample treated with PF-00477736 (Fig. 4c, left panel). Conversely, in MAVER-1 cells only a slightly increased percentage of dUTP-positive cells after drug combination was observed (11%) as compared with untreated cells or cells treated with the single drugs (Fig. 4c, right panel).

Considering the long-lasting cell cycle block in MAVER-1 cells, we next investigated cell cycle perturbation at later timepoints. As shown in Electronic Supplementary Material Figure 3, the block in all cell cycle phases persisted up to 120 h and after this timepoint cells started re-growing, as demonstrated by the growth curve and the DNA histogram at 144 h. The amount of sub-G1 events and apoptotic cells detected by TUNEL assay (not shown) was very low (about 10%), further corroborating the fact that the synergistic effect was mainly cytostatic. A decrease in the phosphorylated levels of ERK1 24 h after the drug combination suggested that the arrest in cell proliferation in this cell line may be mediated by inhibition of the MAPK pathway (Electronic Supplementary Material Figure 4A). Additionally, in MAVER-1 cells there was clear upregulation of p21 expression starting from 24 h and more evident after 48 h of treatment with the combination

(Electronic Supplementary Material Figure 4B), further suggesting inhibition of cell cycle progression. Conversely, in the MINO cells phosphorylation of ERK was inhibited after ibrutinib treatment, while the drug combination partially reversed this effect. No induction of p21 expression was observed in MINO cells (Electronic Supplementary Material Figure 4C–D). These data suggest that the molecular mechanisms at the basis of the synergism in sensitive and resistant cell lines to ibrutinib are different. Induction of apoptosis (caspase-3 activity) was more evident in another ibrutinib-sensitive cell line, JEKO-1, as compared to the ibrutinib-resistant cell line GRANTA-519 after the drug combination (Electronic Supplementary Material Figure 5).

3.4 mRNA Expression of Nuclear Factor-κB Target Genes in Ibrutinib-Sensitive and -Resistant Cell Lines after Combined Treatment

Since ibrutinib affects the NF-κB pathway, we investigated how the expression of the NF-κB target genes was affected by the single and combined treatments in MINO and MAVER-1 cell lines after 24 and 48 h. As previously described [13], ibrutinib leads to downregulation of the NF-κB target genes *TNFAIP3* and *NFKB1A* in the ibrutinib-sensitive cell line MINO, but not in the resistant cell line MAVER-1. PF-00477736 did not affect the expression of these genes in either cell line. In MINO cells the combined treatment downregulated these targets similarly to ibrutinib alone, while in MAVER-1 cells these genes were upregulated by the combination (up to three-fold at 24 h and more than six-fold at 48 h compared with untreated and single drug-treated cells) (Fig. 5).

We also investigated the expression of NF-κB target genes involved in anti-apoptotic and survival pathways (*BCL2*, *BCLXL*, and *BIRC5*) (Fig. 5). The drug combination upregulated the expression of these genes (up to four-fold at 24 h and up to seven-fold at 48 h after treatment compared to untreated and single-treated cells) in MAVER-1, possibly accounting for the lower degree of apoptosis induction observed here. Conversely, there was no substantial effect on the expression of these genes in MINO cells after single or combined treatments.

4 Discussion

MCL is an incurable form of non-Hodgkin lymphoma with a very poor prognosis. The disease is aggressive in the majority of cases with a poor response to therapy in relapsed tumors, so new therapeutic approaches are urgently needed. Recently, with novel technical approaches, the knowledge of the molecular mechanisms involved in the pathogenesis and clinical progression of MCL has improved, leading to the identification of targets for specific targeted molecular therapies. New
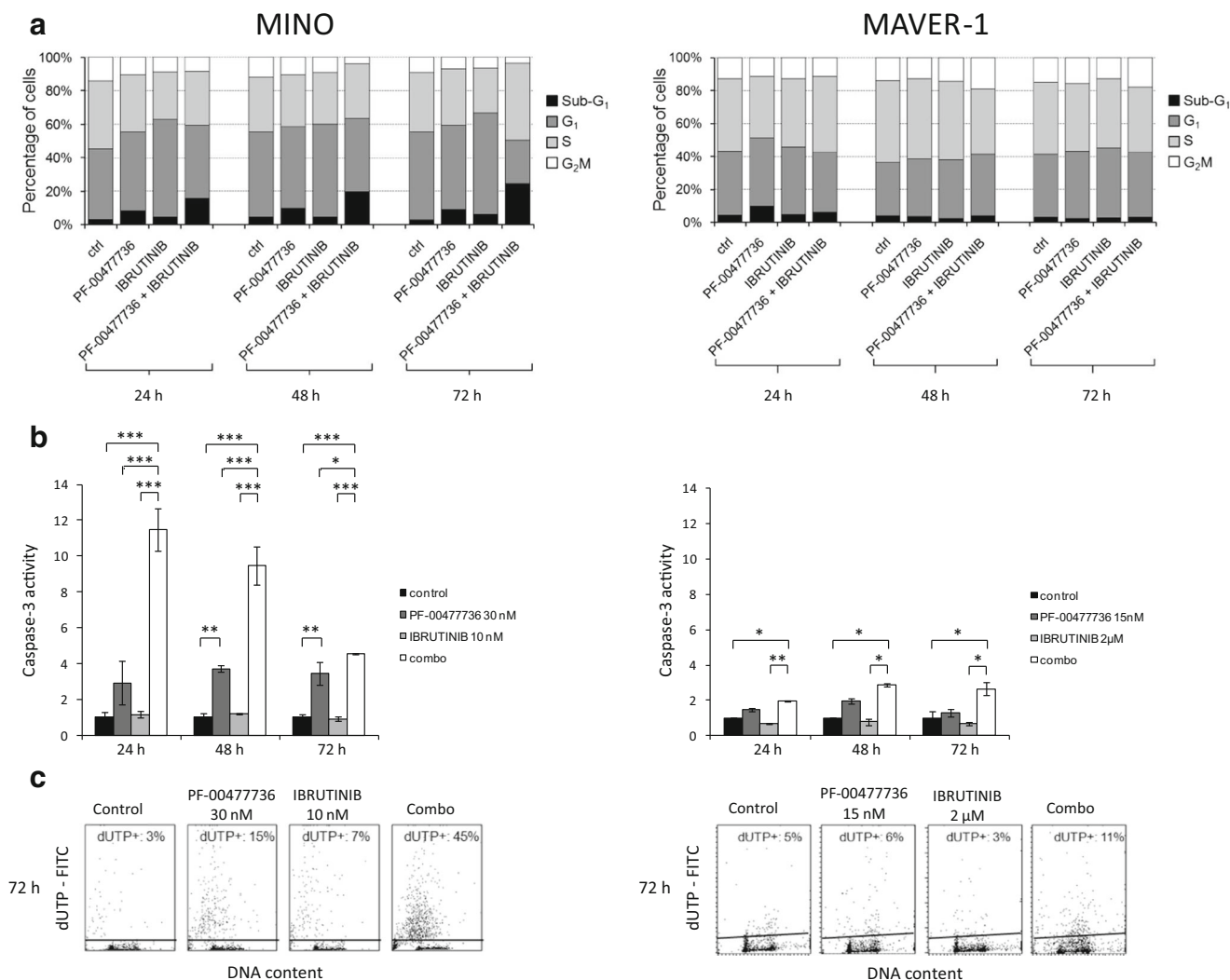
Fig. 4 Cell cycle perturbation and cell death induced by dual BTK and Chk1 inhibition in MINO and MAVER-1 cell lines. **a** Flow cytometric analysis of DNA content after 24, 48, and 72 h of treatment with PF-00477736 and ibrutinib either singly or combined. **b** Caspase-3 activity assay 24, 48, and 72 h after treatment with the two drugs either singly or combined. Data are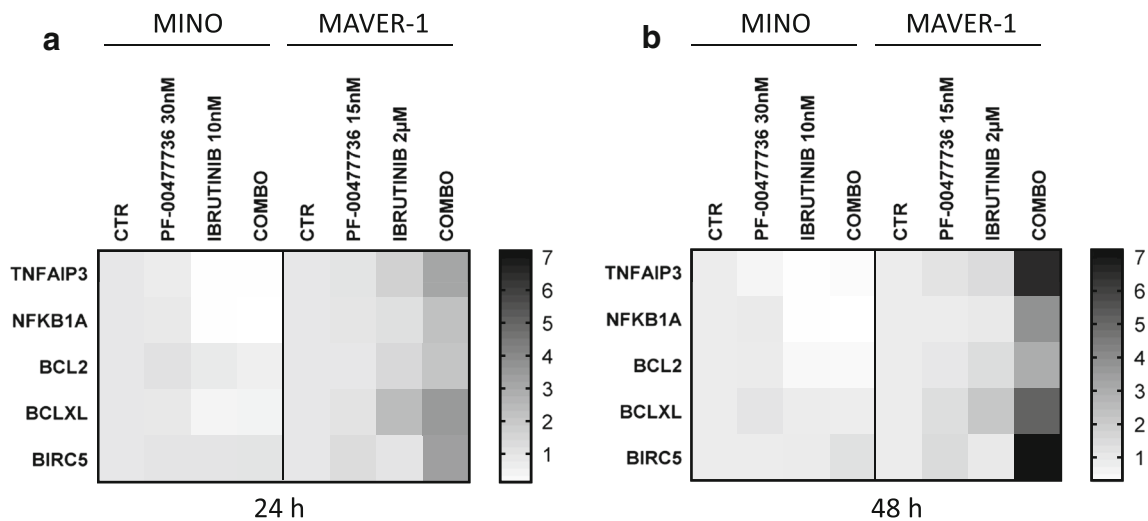 expressed as fold difference from untreated cells and are representative of three independent experiments, as the mean ± standard deviation (SD) of three replicates. The significance of differences was measured with the Student's t-test ($P < 0.05$ was considered statistically significant). * $P < 0.05$, ** $P < 0.01$, *** $P < 0.001$. **c** TUNEL (TdT-mediated dUTP nick-end labeling technique) assay 72 h after treatment with the drugs singly or combined. ctrl control

therapeutic agents have been licensed for relapsed/refractory MCL, such as bortezomib, lenalidomide, temsirolimus, and ibrutinib, while some others are in early clinical trials including BCL2 inhibitors, PI3Kinase inhibitors, and agents involved in immune-checkpoint blockade [21–23].

The BTK inhibitor ibrutinib has been shown to be effective and well-tolerated [9], although primary and secondary resistance often arise in MCL. Patients with relapsed MCL resistant to ibrutinib have a very poor outcome, with low response rates to salvage therapy and a short duration of response [24, 25]. Thus, finding new therapeutic approaches to overcome ibrutinib resistance and/or increase the response is currently an intense area of investigation.

Herein we provide, for the first time, experimental preclinical evidence that interference in the cell cycle checkpoint pathway with Chk1 inhibitors and in the pro-survival pathway with the BTK inhibitor ibrutinib is a very effective pharmacological approach in MCL. The activity of ibrutinib was strongly potentiated (from two to 50 times) by very low concentrations of the Chk1 inhibitor PF-00477736 in all MCL cell lines tested. Interestingly, the potentiation was stronger in MCL cell lines moderately sensitive to ibrutinib (MINO and JEKO-1) than in the very sensitive cell lines (REC-1 and SP49). In the ibrutinib-resistant cell lines the potentiation of the activity of ibrutinib by PF-00477736 was also evident, but at high concentrations of ibrutinib (μM range), much higher than the ones clinically achievable [9, 26].

Fig. 5 Heat maps representing the expression of NF-κB target genes. Relative mRNA levels represented as heat maps showing the expression of the NF-κB target genes *TNFAIP3*, *NFKB1A*, *BCL2*, *BCLXL*, and *BIRC5* in MINO (**a**) and MAVER-1 (**b**) cells after 24 and 48 h of treatment with the drugs either alone or combined. Data are normalized to the internal mRNA levels of actin and are represented as the fold differences from untreated samples at each timepoint. The heat map was obtained with GraphPad Prism 7.0. Data are representative of three independent experiments and are the mean ± standard deviation (SD) of three biological replicates. Statistical significance differences were measured with the Student's t-test ($P < 0.05$ was considered statistically significant), * $P < 0.05$, ** $P < 0.01$, *** $P < 0.001$. MINO—TNFAIP3: ibrutinib and combination (combo) vs. control (CTR) group, *** $P < 0.001$ at both timepoints; combo vs. PF-00477736, *** $P < 0.001$ at both timepoints; NFKB1A: ibrutinib and combo vs. CTR group, ** $P < 0.01$ at both timepoints; combo vs. PF-0047736, ** $P < 0.01$ at 24 h and *** $P < 0.001$ at 48 h; BCL2: ibrutinib vs. control, * $P < 0.05$ at 48 h; combo vs. CTR, * $P < 0.05$ at 24 h and ** $P < 0.01$ at 48 h; combo vs. PF-00477736, ** $P < 0.01$ at 24 h and * $P < 0.05$ at 48 h; BCLXL: ibrutinib and combo vs. CTR, *** $P < 0.001$ at 24 h; combo vs PF-00477736, *** $P < 0.001$ at 24 h and * $P < 0.05$ at 48 h; BIRC5: combo vs. all the other groups, * $P < 0.05$ at 48 h. MAVER-1—TNFAIP3 and NFKB1A: ibrutinib vs. CTR, * $P < 0.05$ at 24 h and ** $P < 0.01$ at 48 h; combo vs. all the other groups: ** $P < 0.01$ at 24 and 48 h; BCL2: PF-00477736 vs. CTR, * $P < 0.05$ at 48 h; ibrutinib vs. CTR, ** $P < 0.01$ at 24 and 48 h; combo vs. all the other groups, ** $P < 0.01$ at 24 h and *** $P < 0.001$ at 48 h; BCLXL: PF-00477736 vs. CTR, * $P < 0.05$ at 24 h and ** $P < 0.01$ at 48 h; ibrutinib vs. CTR, ** $P < 0.01$ at both timepoints; combo vs. PF-00477736 and CTR, *** $P < 0.001$ at 24 h and ** $P < 0.01$ at 48 h; combo vs. ibrutinib: ** $P < 0.01$ at both timepoints; BIRC5: PF-00477736 vs. CTR, ** $P < 0.01$ at both timepoints; combo vs. all the other groups, *** $P < 0.001$ at both timepoints

The ibrutinib-sensitive cell line MINO and the resistant cell line MAVER-1 were investigated in detail to clarify the molecular mechanisms at the basis of the synergism after treatment with PF-00477736 and ibrutinib. The drug combination causes cell proliferation arrest and induces activation of DNA damage response in both cell lines. Activation of apoptosis was more marked in MINO than in MAVER-1 cells. Since both cell lines display mutations in p53 (IARC [International Agency for Research on Cancer] TP53 database), these events are independent of p53. The p21 induction observed in MAVER-1 cells may be responsible for the persistent general cell cycle block in all phases after the drug combination, and may be mediated by the activity of the NF-κB transcription factor, as already observed in other cancer cell lines in response to ionizing radiation (IR) or etoposide [27]. Following treatment with ibrutinib we observed inhibition of p-ERK in the ibrutinib-sensitive cell line but not in the ibrutinib-resistant one, suggesting that this may be correlated with the cell sensitivity to ibrutinib, as previously reported [28]. The drug combination leads to a decrease in p-ERK in MAVER-1 cells, which is possibly related to the general arrest in cell proliferation observed. Conversely,

one might hypothesize that the partial restoration of ERK activity observed after the drug combination in MINO cells could be an important determinant of synergism associated with apoptosis activation in this experimental system [29, 30].

In the MAVER-1 cell line the drug combination upregulated NF-κB target genes, many of which (BIRC5, BCL2, and BCLXL) have specific anti-apoptotic and pro-survival functions, which may explain why apoptosis was only slightly activated in this cell line. We speculate that the upregulation of these NF-κB target genes after dual BTK/Chk1 inhibition in the ibrutinib-resistant MAVER-1 cell line might be due to two events: (1) BTK inhibition does not interfere with the NF-κB pathway because of the presence of an alternative NF-κB pathway, which is constitutively active in these cells [13]; and (2) concomitant Chk1 inhibition may increase NF-κB activity through the lack of negative phosphorylation of the regulatory subunit of the canonical NF-κB pathway relA/p65 at position T505, which is mediated by Chk1 following DNA damage [31]. Unfortunately, we were not able to corroborate this hypothesis for the lack of functionally active, commercially available antibodies against pT505 relA/p65. In ibrutinib-resistant cells the drug combination blocks the cell cycle and arrests cell

proliferation, but it is not able to turn off the NF-κB pathway, hampering the full activation of apoptosis. These data support the hypothesis that in ibrutinib-resistant cells an interference with other pro-survival pathways (the observed reduction in ERK phosphorylation could be one example) may be occurring after the drug combination.

Considering the high ibrutinib concentrations necessary to elucidate a synergistic effect with Chk1 inhibitors in ibrutinib-resistant cell lines, the synergism and the cellular and molecular effects observed in these cell lines are likely due to unknown off-target effects of ibrutinib.

5 Conclusion

In conclusion, we found that combining ibrutinib with Chk1 inhibitors was synergistically active in ibrutinib-sensitive cell lines, inducing cell death by apoptosis, and in ibrutinib-resistant cell lines through a strong arrest of cell growth. However, as the ibrutinib concentrations used to see the synergism in resistant cells lines exceed those clinically achievable in MCL patients, this new combination approach can be considered a promising therapeutic approach only in ibrutinib-sensitive MCL patients.

Despite the limitation given by the lack of testing this drug combination in a primary MCL sample and/or patient-derived xenografts, these findings suggest that simultaneous interference with different, inter-related growth control pathways important for MCL survival (such as the cell cycle checkpoint and pro-survival pathways) is feasible and very effective.

Compliance with Ethical Standards

Conflict of Interest The authors declare no competing financial interests.

References

1. Vogt N, Dai B, Erdmann T, Berdel WE, Lenz G. The molecular pathogenesis of mantle cell lymphoma. Leuk Lymphoma. 2017;58(7):1530–7.
2. Dreyling MH, Bullinger L, Ott G, Stilgenbauer S, Muller-Hermelink HK, Bentz M, et al. Alterations of the cyclin D1/p16-pRB pathway in mantle cell lymphoma. Cancer Res. 1997;57(20): 4608–14.
3. Quintanilla-Martinez L, Davies-Hill T, Fend F, Calzada-Wack J, Sorbara L, Campo E, et al. Sequestration of p27Kip1 protein by cyclin D1 in typical and blastic variants of mantle cell lymphoma (MCL): implications for pathogenesis. Blood. 2003;101(8):3181–7.
4. Camacho E, Hernandez L, Hernandez S, Tort F, Bellosillo B, Bea S, et al. ATM gene inactivation in mantle cell lymphoma mainly occurs by truncating mutations and missense mutations involving the phosphatidylinositol-3 kinase domain and is associated with increasing numbers of chromosomal imbalances. Blood. 2002;99(1):238–44.
5. Bea S, Ribas M, Hernandez JM, Bosch F, Pinyol M, Hernandez L, et al. Increased number of chromosomal imbalances and high-level DNA amplifications in mantle cell lymphoma are associated with blastoid variants. Blood. 1999;93(12):4365–74.
6. Campo E, Rule S. Mantle cell lymphoma: evolving management strategies. Blood. 2015;125(1):48–55.
7. Saba NS, Liu D, Herman SE, Underbayev C, Tian X, Behrend D, et al. Pathogenic role of B-cell receptor signaling and canonical NF-kappaB activation in mantle cell lymphoma. Blood. 2016;128(1):82–92.
8. Baran-Marszak F, Boukhiar M, Harel S, Laguillier C, Roger C, Gressin R, et al. Constitutive and B-cell receptor-induced activation of STAT3 are important signaling pathways targeted by bortezomib in leukemic mantle cell lymphoma. Haematologica. 2010;95(11): 1865–72.
9. Wang ML, Rule S, Martin P, Goy A, Auer R, Kahl BS, et al. Targeting BTK with ibrutinib in relapsed or refractory mantle-cell lymphoma. N Engl J Med. 2013;369(6):507–16.
10. Zhang SQ, Smith SM, Zhang SY, Lynn Wang Y. Mechanisms of ibrutinib resistance in chronic lymphocytic leukaemia and non-Hodgkin lymphoma. Br J Haematol. 2015;170(4):445–56.
11. Colomer D, Campo E. Unlocking new therapeutic targets and resistance mechanisms in mantle cell lymphoma. Cancer Cell. 2014;25(1):7–9.
12. Chiron D, Di Liberto M, Martin P, Huang X, Sharman J, Blecua P, et al. Cell-cycle reprogramming for PI3K inhibition overrides a relapse-specific C481S BTK mutation revealed by longitudinal functional genomics in mantle cell lymphoma. Cancer Discov. 2014;4(9):1022–35.
13. Rahal R, Frick M, Romero R, Korn JM, Kridel R, Chan FC, et al. Pharmacological and genomic profiling identifies NF-kappaB-targeted treatment strategies for mantle cell lymphoma. Nat Med. 2014;20(1):87–92.
14. Chila R, Basana A, Lupi M, Guffanti F, Gaudio E, Rinaldi A, et al. Combined inhibition of Chk1 and Wee1 as a new therapeutic strategy for mantle cell lymphoma. Oncotarget. 2015;6(5):3394–408.
15. Restelli V, Chila R, Lupi M, Rinaldi A, Kwee I, Bertoni F, et al. Characterization of a mantle cell lymphoma cell line resistant to the Chk1 inhibitor PF-00477736. Oncotarget. 2015;6(35):37229–40.
16. Carrassa L, Chila R, Lupi M, Ricci F, Celenza C, Mazzoletti M, et al. Combined inhibition of Chk1 and Wee1: in vitro synergistic effect translates to tumor growth inhibition in vivo. Cell Cycle. 2012;11(13):2507–17.
17. Carrassa L, Sanchez Y, Erba E, Damia G. U2OS cells lacking Chk1 undergo aberrant mitosis and fail to activate the spindle checkpoint. J Cell Mol Med. 2009;13(8A):1565–76.
18. Ubezio P. Microcomputer experience in analysis of flow cytometric DNA distributions. Comput Programs Biomed. 1985;19(2-3):159–66.
19. Honigberg LA, Smith AM, Sirisawad M, Verner E, Loury D, Chang B, et al. The Bruton tyrosine kinase inhibitor PCI-32765 blocks B-cell activation and is efficacious in models of autoimmune disease and B-cell malignancy. Proc Natl Acad Sci U S A. 2010;107(29):13075–80.
20. Leung-Pineda V, Ryan CE, Piwnica-Worms H. Phosphorylation of Chk1 by ATR is antagonized by a Chk1-regulated protein phosphatase 2A circuit. Mol Cell Biol. 2006;26(20):7529–38.
21. Goy A. Mantle cell lymphoma: is it time for a new treatment paradigm? Hematol Oncol Clin North Am. 2016;30(6):1345–70.

22. Inamdar AA, Goy A, Ayoub NM, Attia C, Oton L, Taruvai V, et al. Mantle cell lymphoma in the era of precision medicine-diagnosis, biomarkers and therapeutic agents. Oncotarget. 2016;7(30):48692–731.

23. Tucker D, Rule S. Novel agents in mantle cell lymphoma. Expert Rev Anticancer Ther. 2017;17(6):491–506.

24. Cheah CY, Chihara D, Romaguera JE, Fowler NH, Seymour JF, Hagemeister FB, et al. Patients with mantle cell lymphoma failing ibrutinib are unlikely to respond to salvage chemotherapy and have poor outcomes. Ann Oncol. 2015;26(6):1175–9.

25. Martin P, Maddocks K, Leonard JP, Ruan J, Goy A, Wagner-Johnston N, et al. Postibrutinib outcomes in patients with mantle cell lymphoma. Blood. 2016;127(12):1559–63.

26. Marostica E, Sukbuntherng J, Loury D, de Jong J, de Trixhe XW, Vermeulen A, et al. Population pharmacokinetic model of ibrutinib, a Bruton tyrosine kinase inhibitor, in patients with B cell malignancies. Cancer Chemother Pharmacol. 2015;75(1):111–21.

27. Wuerzberger-Davis SM, Chang PY, Berchtold C, Miyamoto S. Enhanced G2-M arrest by nuclear factor-{kappa}B-dependent p21waf1/cip1 induction. Mol Cancer Res. 2005;3(6):345–53.

28. Zheng X, Ding N, Song Y, Feng L, Zhu J. Different sensitivity of germinal center B cell-like diffuse large B cell lymphoma cells towards ibrutinib treatment. Cancer Cell Int. 2014;14(1):32.

29. Tang D, Wu D, Hirao A, Lahti JM, Liu L, Mazza B, et al. ERK activation mediates cell cycle arrest and apoptosis after DNA damage independently of p53. J Biol Chem. 2002;277(15):12710–7.

30. Cagnol S, Chambard JC. ERK and cell death: mechanisms of ERK-induced cell death–apoptosis, autophagy and senescence. FEBS J. 2010;277(1):2–21.

31. Rocha S, Garrett MD, Campbell KJ, Schumm K, Perkins ND. Regulation of NF-kappaB and p53 through activation of ATR and Chk1 by the ARF tumour suppressor. EMBO J. 2005;24(6):1157–69.